A Computational Study of the Symmetry of an Aluminophosphate Microporous Material. Incorporation of Iron Defects in Aluminum Tetrahedral Sites

Jorge Gulín-González*,† and Carlos de las Pozas del Río‡

Dpto. de Física, Instituto Superior Politécnico José A. Echeverría (ISPJAE), Calle 127 s/n. Apartado 6028, Habana 6, Marianao, La Habana, Cuba, and Division of Chemistry (CNIC), National Center for Scientific Research, P.O. Box 6990, La Habana, Cuba

Received February 16, 2001. Revised Manuscript Received December 18, 2001

A computational study using classical Gibbs free energy minimization techniques of the $AlPO_4$-5 unit cell symmetry is presented. The Gibbs free energy calculations were performed at temperatures up to 600 K. It was found that the orthorhombic *Pcc*2 and the hexagonal *P*6 structures are energetically favored with respect to the *P*6*cc* structure at temperatures up to 400 K. At $T = 500$ K, the hexagonal *P*6*cc* structure has a very slightly lower energy than that obtained for the *P*6 and *Pcc*2 structures. However, the analysis of the vibrational modes reveals the existence of imaginary eigenvalues, which indicates that the space group *P*6*cc* does not describe correctly the unit cell of calcined $AlPO_4$-5. Moreover, the incorporation of iron defects in tetrahedral aluminum sites of the $AlPO_4$-5 unit cell was studied by minimization techniques. It seems probable that iron as Fe^{3+} incorporates in the aluminum tetrahedral sites. Subsequently, several configurations of two and three Fe^{3+} ions in the $AlPO_4$-5 unit cell were studied. The analysis of the most stable configurations highlights the influence of two factors in the stability of FAPO-5 structure: the interaction between the Fe^{3+} ions and the rigidity of the $AlPO_4$-5 unit cell in the *c* direction. The combination of these factors leads to a low stability of the structures with all of the Fe^{3+} ions in the same side of the unit cell and with the ions very close.

1. Introduction and Scope

The problem of the symmetry of the $AlPO_4$-5 unit cell has been the subject of a variety of studies since the synthesis of this material in 1982[1]. The $AlPO_4$-5 possesses a one-dimensional 12 membered channel, which is surrounded by four and six rings (see Figure 1). The 12-membered channel permits the adsorption of large molecules (e.g., hydrocarbons) and its use as catalysts. Initially the as-synthesized structure was refined in a hexagonal space group *P*6*cc*.[2,3] This space group gives a good description of the channel structure, but one of the oxygen sites has a rather large temperature factor and the Al−O−P angles involving this oxygen are close to 180°. Bennet et al.[2] attribute this fact to static disorder of the oxygen which is structurally distributed about three equivalent sites. Richardson et al.[4] in a neutron diffraction study of the calcined sample report that a higher hexagonal symmetry of *P*6/*mcc* was required to obtain a satisfactory refinement, but this model considers a random alternation of the Al and P on the tetrahedral sites, which is contrary to what was found in the experiment. The NMR experiment[5] suggests a lower symmetry than that reported from initial crystallographic study (*P*6*cc*).

Other structure determinations alluded the possible alternatives to space group *P*6*cc*. Ohnishi et al.[6] have reported a reversible phase transition from hexagonal to orthorhombic symmetry in the presence of the tropine. Mora et al.[7] using high-resolution X-ray and neutron powder diffraction have found that between room-temperature and 363 K the $AlPO_4$-5 structure is best described with the orthorhombic space group *Pcc*2. Recently, Klap et al.[8] have determined from single-crystal X-ray diffraction data that the crystal structure of $AlPO_4$-5 is described as consisting of three types of microdomains, each exhibiting P6 symmetry. The domains are related by two sets of glide planes, and the average structure has *P*6*cc* symmetry.

Many theoretical studies have suggested that the symmetry of $AlPO_4$-5 is lower than *P*6*cc*.[9−11] The theoretical predictions of Henson et al.[10] confirm the

* To whom correspondence should be addressed. E-mail: gulin@electrica.ispjae.edu.cu.
† Instituto Superior Politécnico José A. Echeverría (ISPJAE).
‡ National Center for Scientific Research.

(1) Wilson, S. T.; Lok, B. M.; Messina, C. A.; Cannan, T. R.; Flanigen, E. M. *J. Am. Chem. Soc.* **1982**, *104*, 1146.
(2) Bennett, J.; Cohen, J. P.; Flanigen, E. M.; Pluth, J. J.; Smith, J. V. *Intrazeolite Chemistry*; American Chemical Society: Washington, DC, 1983.
(3) Qiu, S.; Pang, Q.; Kessler, H.; Guth, J. L. *Zeolites* **1989**, *8*, 440.
(4) Richardson, J. W.; Pluth, J.; Smith, J. V. *Acta Crystallogr. C.* **1987**, *43*, 1469.
(5) Peeters, M. P.; van de Ven, L.; de Haan, J. W.; van Hooff, J. H. *J. Phys. Chem*. **1993**, *97*, 9254.
(6) Ohnishi, N.; Qiu, S.; Terasaki, O.; Kajitani, T.; Hiraga, K. *Microporous Mater*. **1992**, *2*, 73.
(7) Mora, A. J.; Fitch, A. N.; Cole, M.; Goyal, R.; Jones, R. H.; Jobic, H.; Carr, S. W. *J. Mater. Chem*. **1996**, *6*, 1831.
(8) Klap, G. J.; van Koningsveld; Graafsma, H.; Schreurs, A. M. M. *Microporous Mesoporous Mater*. **2000**, *38*, 403.
(9) de Man, A. J. M.; Jacobs, W. P. J. H.; Gilson, J. P. W.; van Santen, R. A. *Zeolites* **1992**, *12*, 826.
(10) Henson, N. J.; Cheetham, A. K.; Gale, J. D. *Chem. Mater*. **1996**, *8*, 664.

10.1021/cm0101428 CCC: $22.00
Published on Web 05/25/2002

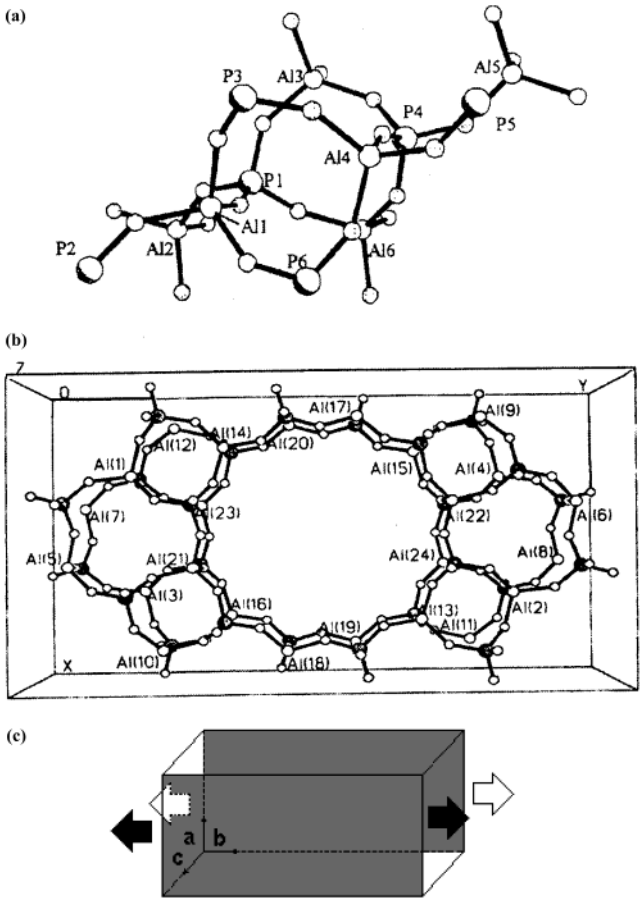

Figure 1. Tetrahedral aluminum sites in $AlPO_4$-5: (a) in asymmetric unit cell and (b) in symmetric unit cell. (c) An ideal representation of the orthorhombic *Pcc*2 unit cell with unit cell parameters *a*, *b*, and *c*. The plane *ab* is represented in gray. Two black (or white) arrows indicate the deformation in this plane when the substitution occurs in the same side of unit cell. One black and white arrow indicate the deformation when the substitution occurs on the opposite side.

presence of a lower symmetry. These authors have demonstrated that a hexagonal unit cell with space group *P*6 is energetically more favored and contains no linear Al−O−P angles. Ruiz-Salvador et al.[11] using minimization methods showed the reduction of the $AlPO_4$-5 symmetry from *P*6*cc* to *P*6. This reduction leads to the relaxation of Al−O−P angles in agreement with the results of Henson et al.[10] Ruiz- Salvador et al.[11] have also determined that the orthorhombic space group *Pcc*2 has an energy similar to that calculated for the *P*6 structure. All of the calculations were made at 0 K.

Richardson et al.[12] in their crystallographic studies about the siliceous analogue of the $AlPO_4$-5 (SSZ-24), found a high-low displacive transition near 370 K. In this paper, the complete refinement of the room-temperature data in the space group *P*6*cc* was possible. However, the two sets of high-temperature data (370 and 464 K) yielded excellent refinements with the hexagonal symmetry.

The substitution of framework atoms in AlPOs leads to materials with new properties (MeAPO). For example, aluminum can be replaced by metals to form MeAPO,[13] such as FAPO,[13−15] CoAPO,[16] etc., and phosphorus can be replaced by silicon to form the silicoaluminophosphate family (SAPO).[17]

Several experimental and theoretical studies about the distribution of different metals over the tetrahedral sites have been performed.[18−22] The structure of a MeAPO[21] was determined by direct combination of experimental refinement and simulation techniques. Other microporous materials were also studied using this methodology.[20,22−23] In particular, the incorporation of iron in zeolite ZSM-5 was already studied by Lewis et al.,[23] obtaining results in good agreement with the experiment.[24]

FAPO-5 can be synthesized using a variety of templates; typically, amines or quaternary ammonium hydroxides and either Fe^{2+} or Fe^{3+} may be used as the source of iron.[15] Calcination of FAPO-5 materials at 600 °C in air results in oxidation of Fe^{2+} to Fe^{3+}. The degree of incorporation of iron in the AlPO framework seems to be strongly dependent on the method of synthesis and still remains as an open question. Li et al.[14] found that substantial amounts of iron enter the framework by adding an Fe^{2+} salt to the synthesis gel. Wequin et al.[25] also reported that large amounts of iron can be incorporated into the framework if enough iron source is available and detected the presence of both Fe^{2+} and Fe^{3+} in the framework. However, Cardile et al.[18] found that only a small quantity of iron enters the framework. The results of Das et al.[19] revealed an increased substitution of iron (as Fe^{3+} ion) in the $AlPO_4$-5 framework with increased time of reaction. According to the temperature-programmed desorption (TPD) of ammonia experiments of these authors, the presence of the Fe^{2+} in the tetrahedral aluminum sites does not occur.

In this paper, a computational study of the symmetry of the unit cell of $AlPO_4$-5 at variable temperatures and the stability of this structure in the presence of iron (Fe^{2+} and Fe^{3+}) are presented. We have calculated the Gibbs free energies for different space groups of the unit

(11) Ruiz-Salvador, A. R.; Sastre, G.; Lewis, D. W.; Catlow, C. R. A. *J. Mater. Chem*. **1996**, *6*, 1837.
(12) Richardson, J. W., Jr.; Smith, J. V.; Han, S. *J. Chem. Soc., Faraday Trans*. **1990**, *86*, 2341.
(13) Flaningen, E. M.; Lok, B. M.; Patton, R. L. Wilson, S. T. *Proc. 7th Int. Zeolite Conf*; Kodansha Ltd.: Tokyo, 1986.
(14) Li, H. X.; Martens, J. A.; Jacobs, P. A.; Schubert, S.; Schmidt, F.; Zeithen, H. M.; Trautwein, A. X. *Stud. Surf. Sci. Catal.* **1988**, *37*, 75.
(15) Messina, C. A.; Lok, B. M.; Flaningen, E. M. *Eur. Patent Appl.* **1985**, *131*, 946.
(16) Bennett, J. M.; Marcus, B. K. *Stud. Surf. Sci. Catal.* **1988**, *37*, 269.
(17) Lok, B. M.; Messina, C. A.; Patton, R. L.; Gajek, R. T.; Cannan, T. R.; Flanigen, E. M. *J. Am. Chem. Soc.* **1988**, *106*, 6092.
(18) Cardile, E. M.; Tapp, N. J.; Milestone, N. B. *Zeolites* **1990**, *10*, 90.
(19) Das, J.; Satyanaryana, C. V. V.; Chakrabarty, D. K.; Piramanayagam, S. N.; Shringi, S. N. *J. Chem. Soc., Faraday Trans.* **1992**, *88*, 3255.
(20) Gulín-González, J.; de la Cruz Alcaz, J.; Ruiz-Salvador, A. R.; Gómez, A.; Dago, A.; de las Pozas, C. *Microporous Mesoporous Mater.* **1999**, *29*, 361.
(21) Wright, P. A.; Natarjan, S.; Thomas, J. M.; Bell, R. G.; Gai-Boyes, P. L.; Jones, R. H.; Cehn, J. S. *Angew. Chem., Int. Ed. Engl.* **1992**, *31*, 1472.
(22) Gulín-González, J.; de la Cruz Alcaz, J.; López Nieto, J. M.; de las Pozas, C. *J. Mater. Chem*. **2000**, *10*, 2597.
(23) Lewis, D. W.; Catlow, C. R. A.; Sankar, G.; Carr, S. W. *J. Phys. Chem*. **1995**, *99*, 2377.
(24) Axon, S. A.; Barrie, P. J.; Carr, S. W.; Fox, K. K.; Klinowski, J.; *Procceding of the Materials Research Society*; Material Research Society Conference; Materials Reserch Society: Warrendale, PA, 1990; p 51.
(25) Wequin, P.; Shilun, Q.; Qiubin, K.; Zhiyun, W.; Shaoyi, P. *Stud. Surf. Sci. Catal.* **1989**, *49*, 281.

cell (*P*6*cc*, *P*6, and *Pcc*2) and temperatures up to 600 K. Moreover, predictions for the structure and the elastic constants of $AlPO_4$-5 were discussed. Several configurations with one, two, and three atoms of Fe^{3+} were studied.

2. Computational Methodology

Free energy minimization was performed using the code GULP.[26] This program has extensively been used to calculate structural and physical properties of microporous materials.[10,11,20,22,23] The Gibbs free energy calculations were performed using the harmonic approximation. It assumes that vibrational motions in the solids are described by independent quantized harmonic oscillators whose frequencies vary with cell volume. At sufficiently high temperatures, the potential energy surfaces are critically anharmonic, and the application of the harmonic approximation yields inexact results. A good criterion for the election of the maximum temperature where harmonic approximation could be used is half of the melting temperature.[26] In zeolites, the melting temperatures are generally "high" ($T_m \sim$ 1200, 1300 K). To take this fact into account, we have worked with temperatures up to 600 K.

The minimization can be achieved by varying the cell volume and the position of the ions until the configuration satisfies the equilibrium condition. The Gibbs free energy function (G) is related to the Helmholtz free energy (A) through the expression:

$$G = A + PV \tag{1}$$

$$P = P_{ext} - P_{int} \tag{2}$$

In eq 2, P is the total pressure. It has two components: the external pressure applied and the internal pressure due to the phonons. The internal pressure could be calculated by:

$$P_{int} = \partial A/\partial V \tag{3}$$

Assuming the harmonic approximation, the free energy depending on the vibrational entropy by the equation:

$$A = U - TS_{vib} \tag{4}$$

Here, U is the total energy of the unit cell and S_{vib} denotes the vibrational entropy, which can be calculated by:

$$S_{vib} = R \ln Z_{vib} + RT[\partial \ln Z_{vib}/\partial T] \tag{5}$$

where Z_{vib} is the vibrational partition function that can be calculated by:

$$Z_{vib} = \sum_{k-points} W_k \sum_{all\ modes} [1 - \exp(-h\gamma/kT)]^{-1} \tag{6a}$$

Also, the zero point energy (ZPE) can be obtained from:

$$ZPE = \sum_{k-points} W_k + \sum_{all\ modes} h\gamma/2 \tag{6b}$$

where W_k denotes the weight associate with each given k- point in the Brillouin zone.

After the Gibbs free energy is minimized, the thermodynamics properties, the elastic constants, and the structure of the solid can be computed. For the energy minimization of FAPO-5 and the calculation of the defect energy, the shell-model potential was used. The interactions between i and j atoms are represented by a Buckingham potential plus a Coulombic potential:

$$E_{ij} = A_{ij} \exp(-r_{ij}/\rho) - C_{ij}/r^6 + q_i q_j/r_{ij}^2 \tag{7}$$

The long-range interactions are calculated by the Ewald summation,[27] whereas the short-range interactions are calculated using a direct summation. The short-range Buckingham potential is evaluated for a cutoff of 12 Å. The polarizability of the highly polarizable oxygen ions are modeled using a shell model,[28] which comprises rigid cores coupled to the shells by a harmonic spring:

$$E_{core-shell} = 1/2 k_{ij}(r_{core} - r_{shell})^2$$

To make the representation of the covalent bonds more realistic, a bond bending term is also included. The joint use of these potentials in connection with formal ionic charges has been successfully employed in the study of microporous materials,[20−23] although we note that standard molecular mechanic force fields have been employed to model zeolites and related materials.[29,30]

The potential parameters of Gale and Henson were used to model the interactions associated with the AlPO.[31] For the Fe−O interaction, two sets of potential parameters were employed: the potential parameters reported by Sayle et al.[32] and by Lewis and Catlow.[33] All atomic coordinates and cell parameters were optimized to zero forces using the second derivative Newton−Raphson method.[34] Any optimized structures having imaginary phonon frequencies (i.e., a saddle point on the energy surface has been found rather than a minimum) were further optimized using the RFO method,[35] to remove the imaginary modes. A convergence criterion of a gradient norm below 0.001 eV/Å was used for all of the calculations.

We used the Mott-Littleton methodology[36] to treat the incorporation of defects of iron in the framework. This method explicitly relaxes an inner region (region I) with around 500 atoms surrounding the defect to minimum energy. The more distant region (region II) of the crystal is considered as a dielectric continuum. The defect energy calculations were performed with a region I radius of 8 Å and region II radius of 20 Å.

3. Description of the Calculations and Results

3.1. Study of the Temperature-Induced Changes of the $AlPO_4$-5 Structure. First we performed calculations in the structure with hexagonal space group *P*6/

(26) Gale, J. D. *J. Chem. Soc., Faraday Trans.* **1997**, *93*, 629.
(27) Ewald, P. P. *Ann. Phys.* **1921**, *64*, 253.
(28) Dick, B. G.; Overhauser, A. W. *Phys. Rev.* **1958**, *112*, 90.
(29) Lasaga, A. C.; Gibbs, G. V. *Phys. Chem. Miner.* **1987**, *14*, 107.
(30) Smirnov, K. S.; Bougeard, D.; *J. Phys. Chem.* **1993**, *97*, 9434.
(31) Gale, J. D.; Henson, N. J.; *J. Chem. Soc., Faraday Trans.* **1994**, *90*, 3175.
(32) Sayle, D. C.; Catlow, C. R. A; Perrin, M. A.; Nortier, P. *J. Phys Chem. Solids* **1995**, *56*, 799.
(33) Lewis, G. V.; Catlow, C. R. A. *J. Phys. C.* **1985**, *18*, 1149.
(34) Shanno, D. F. *Math. Comput.* **1970**, *24*, 647.
(35) Simons, J.; Jørgensen, P.; Taylor, H.; Ozment, J. *J. Phys. Chem.* **1983**, *87*, 2745.
(36) Mott, N. F.; Littleton, M. J. *Trans. Faraday Soc.* **1938**, *38*, 485.

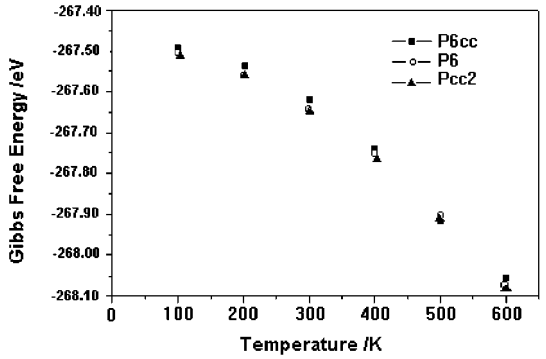

Figure 2. Dependence of the Gibbs free energy on temperature for different $AlPO_4$-5 unit cell. The applied external pressure was 0 GPa.

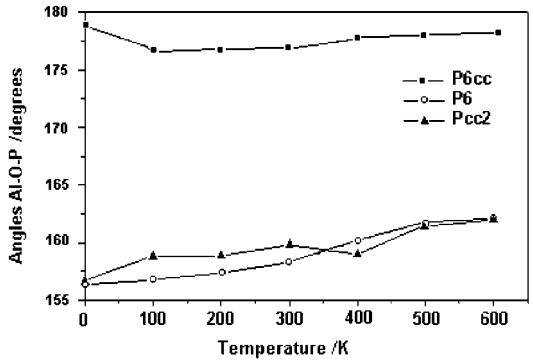

Figure 3. Calculated Al−O−P bond angles at variable temperature for the different $AlPO_4$-5 unit cell. The Al−O−P bond angles are increased ∼1.2° per 100 K.

mcc[4] and considering a random distribution of the aluminum on the tetrahedral sites of the $AlPO_4$-5 unit cell. The main objective was to determine if at 0 K this space group could describe satisfactorily the aluminophosphate structure. The unit cell *P*6/*mcc* retains the linear Al−O−P bond angles in the *c* direction and was proposed as an alternative to the hexagonal space group *P*6*cc*.[4] The random distribution of Al and P on tetrahedral sites has not been experimentally observed in aluminophosphates and leads to the violation of the Löwestein's rule.[37] The energy minimization results at 0 K show that the structure with space group *P*6/*mcc* is unstable with respect to the *P*6*cc*, *Pcc*2, and *P*6 unit cell**.** Therefore, in the following free energy calculations, the *P*6/*mcc* unit cell was not considered.

To investigate the influence of the temperature on the symmetry of the $AlPO_4$-5 unit cell, we calculated the Gibbs free energy for structures with different proposed symmetries of $AlPO_4$-5. The calculations were performed up to 600 K, and we used two starting structures: the orthorhombic *Pcc*2 of Mora et al.[7] (without symmetry unit cell constraint) and the hexagonal *P*6*cc*[2] (with and without symmetry unit cell constraint).

In Figure 2, the dependence of the Gibbs free energy on the temperature is shown. Some comments can be made about this result:

(i) The minimization of the hexagonal *P*6*cc* structure (without symmetry constraint) at temperatures up to 600 K leads to a structure with hexagonal space group *P*6 as has been theoretically reported by Ruiz-Salvador et al.[11] at 0 K. The Hessian matrix (second derivative matrix of the potential function) of the final structure has all eigenvalues positive, and therefore, all of the vibrational frequencies are real. It means that the structure has converged to a true minimum. The structure with the hexagonal space group *P*6 has no linear angles Al−O−P according to the experiment.[7,8] Also, theoretical predictions of Henson et al.[10] have proposed the space group P6 for the description of $AlPO_4$-5 unit cell, and more recently, Klap et al.[8] have experimentally determined that the crystal structure of this aluminophosphate is described as consisting of three types of microdomains, each exhibiting P6 symmetry.

(ii) At temperatures up to 400 K, the orthorhombic *Pcc*2 and the hexagonal *P*6 structures have very similar energies and are energetically favored with respect to the hexagonal *P*6*cc* structure. At 500 K, the *P*6*cc* structure has a slightly lower energy than the *P*6 and *Pcc*2 structures. However, the analysis of the eigenvalues in the *P*6*cc* structure reveals the existence of imaginary frequencies, which means that the calculated energy corresponds to a saddle-point on the energy potential surface. This result confirms that space group *P*6*cc* does not describe correctly the unit cell of the calcined $AlPO_4$-5 according to previous experiments.[7−12]

Table 1. Calculated Unit Cell Parameters for the Orthorhombic *Pcc*2 Cell and the Hexagonal *P*6 Unit Cell at 400 K[a]

unit cell	a/Å	b/Å	c/Å	α/°	β/°	γ/°	V/Å^3
expt[7] (*Pcc*2)	13.794	23.900	8.4168	90	90	90	2775
calcd (*Pcc*2)	13.799	23.980	8.4779	90.01	89.97	90.03	2805
expt[9] (P6)	13.718	13.718	8.4526	90	90	120	1378
calcd (P6)	13.811	13.819	8.4701	90.12	89.97	119.82	1402

[a] Comparison with the experimental *Pcc*2 unit cell of Mora et al.[7] and the experimental *P*6 unit cell of Klap et al.[8]

The calculated Al−O and P−O bond distances and the Al−O−P bond angles at variable temperature for the three different structures are shown in Figure 3. The Al−O−P bond angles are increased with the temperature (∼1.2° per 100 K). The *Pcc*2 and P6 structures present Al−O−P angles between 155 and 160° according to the experiments.[5,7−8] The increase of the Al−O−P bond angles is the cause of the expansion of the unit cell. The Al−O and P−O bond distances are practically temperature independent.

In Table 1, the unit cell parameters for the *P*6 and *Pcc*2 structure at 400 K and the experimentally reported by Mora et al.[7]and Klap et al.[8] are shown. The energy difference between both structures is extremely small ($\Delta E = 0.006$ eV $< kT = 0.04$ eV). The simulated and experimental parameters for the orthorhombic *Pcc*2 structure are very close. Only a small overestimation of the unit cell volume is observed (∼1%).

The vibrational spectrum at 400 K derived from above-described potentials and the IR experimental spectrum[9] of $AlPO_4$-5 are shown in Figure 4. The fundamental frequencies present a reasonable agreement with the experiment. We have not found a remarkable difference between the spectrum at 400 K and at lower temperatures supporting the election of the orthorhombic space group *Pcc*2 at temperatures up to 400 K.

Predictions for the independent elastic constants for the orthorhombic *Pcc*2 unit cell are shown in Table 2.

(37) Löwestein, W. *Am. Miner.* **1954**, *39*, 92.

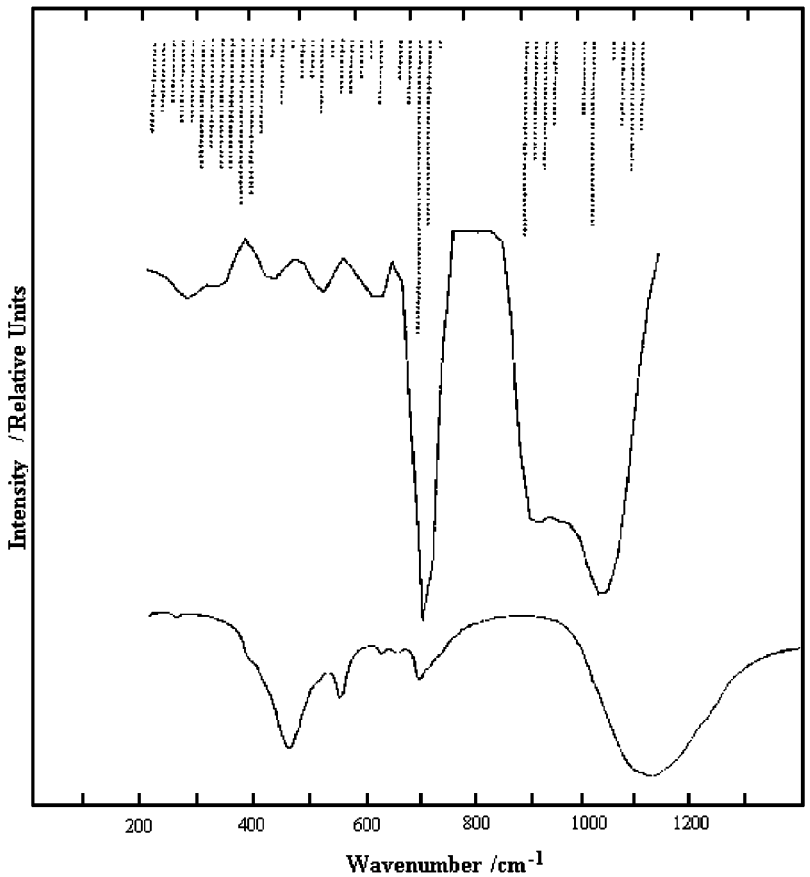

Figure 4. Simulated vibrational spectrum at 400 K and the IR experimental spectrum of $AlPO_4$-5.[9] The simulated spectrum at this temperature does not present the essential difference with the spectrum at 0 K. Because of simulation produce the number of phonon modes per each frequency we have used relative units in the *y* axis. Dotted line represents the numerical calculation performed by GULP program and continuum lines represent: Top: smoothed vibrational spectrum obtained from the numerical calculation. Bottom: IR experimental spectrum of $AlPO_4$-5[9]

Table 2. Predictions for the Elastic Constants in the Orthorhombic *Pcc*2 Structure at 400 K[a]

C_{ij}	value/ 10^{11}dyn/cm^2	C_{ij}	value/ 10^{11}dyn/cm^2
C_{11}	7.53	C_{66}	2.13
C_{22}	7.76	C_{12}	3.28
C_{33}	7.41	C_{13}	0.47
C_{44}	2.48	C_{23}	0.50
C_{55}	2.46		

[a] Calculations were performed using GULP code.[26]

The calculation was performed at $T = 400$ K. An orthorhombic cell has nine independent elastic constants (in general the elastic constants matrix has 6×6 elements C_{ij}). The experimental elastic constants of the $AlPO_4$-5 structure are not available**.** So, its predictions would be very important for a future experimental work and for the understanding of their mechanical properties.

3.2. Iron Defects in Aluminum Tetrahedral Sites of the $AlPO_4$-5 Unit Cell. *3.2.1. Incorporation of the Fe^{2+} and Fe^{3+} Ions in the $AlPO_4$-5 Unit Cell.* The incorporation of the one Fe^{3+} or Fe^{2+} ions in the tetrahedral aluminum sites was studied by energy minimization and defect techniques. The starting point was the orthorhombic unit cell of Mora et al.[7] The potential parameters of Sayle et al.[32] were employed. All of the calculations were performed at 0 K, and no symmetry constraints to the $AlPO_4$-5 unit cell were imposed.

The substitution of aluminum by the Fe^{2+} ion introduces a net negative charge in the framework, which can be compensated by protons or extraframework $Fe^{2+,3+}$ cations. The first mechanism can be described according to the following equation:

$$[AlPO_4] + Fe^{2+} + H^+ \rightarrow [Fe^{2+}, H^+] + Al^{3+} \quad (8)$$

However, the introduction of protons in the structure supposes a certain acid behavior of the FAPO-5 structure, and this has not been experimentally observed.[19] On the other hand, the presence of extraframework Fe^{2+} or Fe^{3+} ions produces a significant distortion of the structure, which is energetic and geometrically unfavorable.

Table 3 shows the calculated substitutional defect energy of an isolated Fe^{2+} and Fe^{3+} in the six independent aluminum sites of the $AlPO_4$-5 unit cell. The appreciable difference obtained for the Fe^{2+} case in comparison with the Fe^{3+} case ($\sim$21 eV) would suggest that the incorporation of Fe^{2+} in tetrahedral sites is very expensive for the $AlPO_4$-5 framework. Another factor to be taken into account is the contribution of the relaxation of the framework. In this respect, we also present in Table 3 the optimized maximum and minimum Fe−O bond distances for both cases (Fe^{2+} and Fe^{3+}). The Fe^{2+}−O is incremented about 0.5−0.6 Å with respect to the experimental Al−O distances in the $AlPO_4$-5 structure. The strong variation in bond dis-

Table 3. Calculated Defect Energy and Calculated Fe−O Bond Distance for the Substitution of One Fe^{2+} and One Fe^{3+} in the Six Nonequivalent Aluminum Sites of the Orthorhombic *Pcc*2 Unit Cell[a]

	substitution by Fe^{2+}		substitution by Fe^{3+}		
site	def. energy/eV	Fe−O distance/Å	def. energy/eV	E/eV[b]	Fe−O/Å
T_1	25.48	2.289−2.346	4.07	−267.5653	2.034−2.058
T_2	25.29	2.245−2.309	4.03	−267.5690	2.030−2.070
T_3	25.44	2.238−2.364	3.96	−267.5638	2.026−2.060
T_4	25.38	2.301−2.358	3.97	−267.5653	2.033−2.059
T_5	25.38	2.271−2.314	4.04	−267.5690	2.032−2.071
T_6	25.47	2.250−2.369	4.07	−267.5638	2.027−2.061

[a] The potential parameters of Sayle et al.[32] were used. [b] Total energy per AlO_4 unit of $AlPO_4$-5.

tances and angles means that the $AlPO_4$-5 framework does not easily accept the incorporation of the Fe^{2+} ion in the aluminum tetrahedral sites, in agreement with the experiments.[18, 19] In contrast, the Fe^{3+} ion is accommodated very well by the $AlPO_4$-5 structure. Considering this result, we will work on what follows using only the Fe^{3+} case.

For the calculation of the dissolution energy of the Fe_2O_3 in the $AlPO_4$-5 structure, we have constructed the following Born−Haber cycle. The experimental source considered for the Fe^{3+} ions was the Fe_2O_3, according to the experiment.[19]

Thus

$$[AlPO_4] + Fe_2O_3 \rightarrow [2Fe]_{Al,Al} + Al_2O_3 \qquad (9)$$

Here $[2Fe]_{Al,Al}$ represents the substitution of two Fe^{3+} ions in aluminum tetrahedral sites of the $AlPO_4$-5 unit cell.

The dissolution energy is then

$$\Delta E_{2Fe} = E_{2Fe} + E_{latt}(Al_2O_3) - E_{latt}(Fe_2O_3) \qquad (10)$$

The first term on the right-hand side is the defect energy of two noninteracting Fe^{3+}, and the energies of the eq 9 are referred to the following processes:

$$Fe_2O_3 \rightarrow 2Fe^{3+} + 3O^{2-}$$
$$-E_{latt}(Fe_2O_3) = +65.79 \text{ eV/(mol of } Fe_2O_3)$$

$$[AlPO_4] + 2Fe^{3+} \rightarrow [2Fe]_{Al,Al} + 2Al^{3+}$$
$$E_{2Fe} = +7.93 \text{ eV}$$

$$2Al^{3+} + 3O^{2-} \rightarrow Al_2O_3$$
$$E_{latt}(Al_2O_3) = -80.32 \text{ eV/(mol of } Al_2O_3)$$

The dissolution energy calculated by eq 9 is negative (−3.30 eV per Fe^{3+} ion) indicating that a considerable amount of Fe_2O_3 is dissolved in the aluminum tetrahedral sites.

To confirm the incorporation of the Fe^{3+}, the simulation of the FAPO-5 was performed using another set of potential parameters (Lewis−Catlow[33]). The results with both parameter sets are qualitatively similar, but some differences in bond distances and angles were obtained. The analysis of the total energies of the different structures reveals that the sites T_2 and T_5 are the most probable for the incorporation of Fe^{3+} (the tetrahedral aluminum sites in the asymmetric and symmetric $AlPO_4$-5 unit cell are shown in Figure 1 parts a and b, respectively). In both cases, the angles and the bond lengths are markedly affected by the incorporation of the metal, as it has been previously reported.[22−24, 39]

Table 4. Calculated Unit Cell Parameters for the Most Stable Sites (T_2 and T_5) with one Fe^{3+} in Tetrahedral Aluminum Sites of $AlPO_4$-5 Unit Cell

potential	a/Å	b/Å	c/Å	α/°	β/°	γ/°	V/Å^3
Sayle et al.[32] [a]	13.795	24.024	8.431	90.01	90.10	89.62	2794.1
Lewis−Catlow[33] [a]	13.755	23.970	8.431	90.05	90.10	90.07	2779.8

[a] The energies for the sites T_2 and T_5 are equal up to the 7th significant.

The unit cell parameters and unit cell volume obtained for the configurations with the Fe^{3+} in the sites T_2 and T_5 are shown in Table 4. The unit cell parameters obtained using both parameter sets are very similar. However, in the structure minimized with the Sayle's parameters the angle γ is equal to 89.62 degrees (90.07 degrees for the Lewis- Catlow's potential parameters).

3.2.2. Distribution of Two and Three Fe^{3+} Ions in the Aluminum Tetrahedral Sites of the $AlPO_4$-5 Unit Cell. The presence of more than one Fe^{3+} in the unit cell adds a term of interaction energy between the defects to the total energy of the FAPO-5. The interaction energy between defects depends on the distance between both. If the defects are very far, the energy of interaction between both is practically zero, $\Delta E \approx 0$, and the energy of the two defects will be:

$$E_{2Fe} = 2E_{1Fe-isl} \qquad (11)$$

where $E_{1Fe-isl}$ is the defect energy of the one Fe^{3+} isolated ion and E_{2Fe} is the defect energy of two Fe^{3+} ions.

If the Fe^{3+} ions are very close, the interaction between both is very strong. Then, the energy of interaction is

$$\Delta E_{2Fe} = E_{2Fe} - 2E_{1Fe-isl} \qquad (12)$$

In Figure 5, the histogram of the energies of the 78 nonequivalent configurations of two Fe^{3+} ions, Figure 5a, and the 256 nonequivalent configurations of three Fe^{3+} ions, Figure 5b, in the $AlPO_4$-5 unit cell are shown. The Sayle's potential parameters were used. The distribution of the energies corresponds to the Gaussian function. The energy and unit cell parameters of the five most and least stable configurations of two and three Fe^{3+} ions in the aluminum tetrahedral sites are shown in Tables 5 and 6, respectively. The five most stable configurations of two Fe^{3+} have, at least, one Fe^{3+} in the sites T_2 or T_5 (the most stable sites for one Fe^{3+} ion). After the occupation of these preferable sites (T_2 or T_5), another ion is localized on the opposite sides of the $AlPO_4$-5 unit cell.

On the other hand, the most stable structures with two and three Fe^{3+} ions (T_1-T_{20} and $T_1-T_5-T_{20}$) present unit cell parameters that do not correspond to the initial orthorhombic unit cell of pure $AlPO_4$-5. In particular, the angle γ varies between 90.79 and 91.23°.

4. Critical Discussion

4.1. Symmetry Properties of the $AlPO_4$-5 Unit Cell. The stability of the structure with orthorhombic

(38) Sastre, G.; Lewis, D. W.; Catlow, C. R. A. *J. Phys. Chem.* **1996**, *100*, 6722.
(39) Blasco, T.; Concepción, P.; López Nieto, J. M.; Pérez-Pariente, J. *J. Catal.* **1995**, *152*, 1.

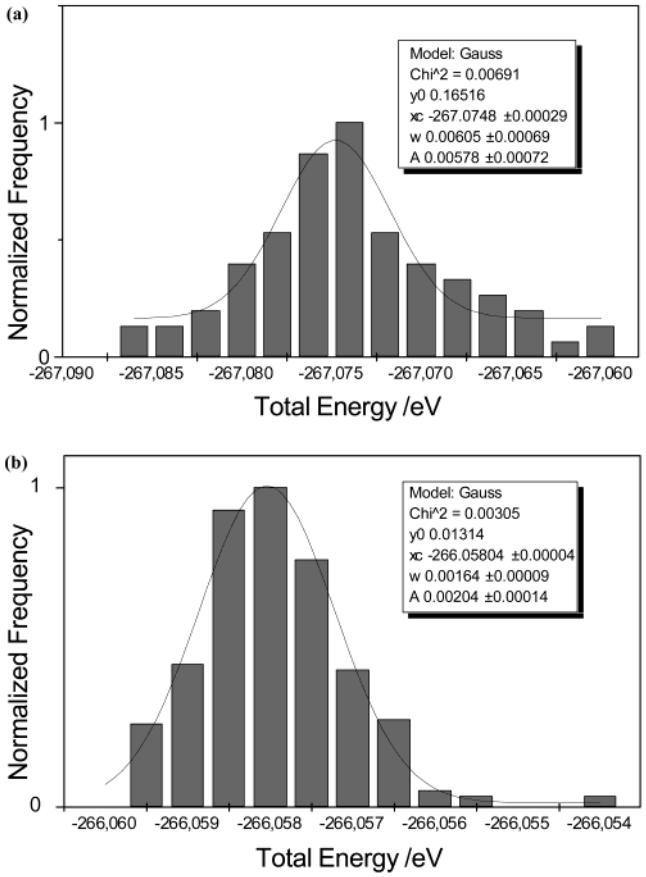

Figure 5. (a) Histogram of the energies of the 78 nonequivalent configurations of two Fe^{3+} in aluminum tetrahedral sites of the $AlPO_4$-5 unit cell. Continuum line: Gaussian fit. (b) Histogram of the energies of the 256 nonequivalent configurations of three Fe^{3+} in aluminum tetrahedral sites of the $AlPO_4$-5 unit cell. Continuum line: Gaussian fit.

Table 5. Energy and Unit Cell Parameters for the Five Most and Least Stable Configurations with Two Fe^{3+} in the Tetrahedral Aluminum Sites of $AlPO_4$-5 Unit Cell[a]

N^b	conf		E/eV[c]	a/Å	b/Å	c/Å	α/°	β/°	γ/°
1	1	20	−267.0838	13.825	24.160	8.4761	89.82	90.20	91.23
2	5	16	−267.0829	13.816	24.178	8.4811	90.22	90.18	88.90
3	1	8	−267.0817	13.820	24.180	8.4888	89.79	90.18	91.05
4	13	20	−267.0817	13.821	24.179	8.4886	89.79	90.18	91.06
5	1	19	−267.0811	13.818	24.190	8.4607	89.91	89.96	91.06
74	5	10	−267.0659	13.904	23.898	8.4910	90.02	90.09	89.70
75	17	22	−267.0659	13.895	23.930	8.4779	90.03	90.05	89.70
76	13	22	−267.0652	13.882	24.012	8.4935	89.78	90.16	90.51
77	1	10	−267.0645	13.864	24.058	8.4926	89.74	90.05	90.62
78	9	22	−267.0606	13.966	23.884	8.4847	89.98	90.02	89.53

[a] Parameters potential of Sayle et al.[32] were used. [b] Rank by Energy. [c] Total energy per AlO_4 unit of $AlPO_4$-5.

space group *Pcc*2 with respect to the structure with hexagonal space group *P*6*cc* is consistent with the experimental results of Richardson et al.[4] at low temperature and with the crystallographic study of Mora et al.[7] at room temperature. Probably, the *P*6*cc* symmetry in $AlPO_4$-5 is possible only as an "average structure" resulting from the combination of the microdomains with less symmetry, according to the experiments of Klap et al.[8]

The extremely small Gibbs free energy difference between the *P*6 and *Pcc*2 structures could suggest a reversible phase transition of the $AlPO_4$-5 unit cell with the temperature. According to our calculations and the experimental results of Richardson et al.,[12] the most probable transition is from an orthorhombic *Pcc*2 to a hexagonal symmetry at "high" temperature (∼ 400, 500 K). However, the experimental results of Richardson et al.[12] were obtained in the all-silica form of the $AlPO_4$-5 (SSZ-24), and the differences between the Si−O−Si and the Al−O−P unit may yield a slightly different behavior with the temperature between both structures, SSZ-24 and $AlPO_4$-5. For example, the transition from α to the β phase in the quartz (SiO_2) and their aluminophosphate analogue, berlinite ($AlPO_4$), takes place at a slightly different temperature ($T \cong 857$ K in $AlPO_4$ and $T \cong 846$ K in SiO_2).[40]

Other space groups have been considered for describing the $AlPO_4$-5 unit cell; in particular, the orthorhombic *Ccc*2 has been extensively treated.[5−7] The election of this space group is supported by two results: It was observed in the $AlPO_4$-5 with tropine organic molecule,[6] and also, the NMR experiments[5] indicate the existence of three crystallographic independent sites in the $AlPO_4$-5 unit cell (as in the space group *Ccc*2). However, the crystallographic study of Mora et al.[7] in the calcined sample reveals the presence of peaks in the diffraction pattern that do not correspond to the C-centered groups. The energy minimization in the space group *Ccc*2 at 0 K was performed, and the final energy obtained is higher than in the space group *Pcc*2 ($E_{Ccc2} = -268.0532$ eV > $E_{Pcc2} = -268.0536$ eV).

4.2. Iron Defects in the $AlPO_4$-5 Structure. The preference of the $AlPO_4$-5 framework by the Fe^{3+} ion is in agreement with a lot experimental results.:[19] Mössbauer spectroscopy, electron paramagnetic resonance (EPR), and temperature-programmed desorption (TPD) of ammonia. On the basis of our simulations, the incorporation of Fe^{2+} is unfavorable from an energetic and geometric point of view. However, the reduction of Fe^{3+} to Fe^{2+} under reaction conditions may be possible as has been previously observed in $AlPO_4$ with the AEL topology.[41]

The deviation of the γ parameter from the initial value, 90°, in the most stable structures with one, two, and three Fe^{3+} ions in aluminum tetrahedral sites could be associated with a change of the $AlPO_4$-5 symmetry because of the incorporation of iron. The phase transition of the AlPO's structures in the presence of different metals (Zn, Mg, Mn, Co, Cr, Cu, and Cd) has been reported recently.[42] According to these authors, the influence of metal on the symmetry and thermal stability of the products is critical**.** They also reported that the amount of the introduced metal plays a more important role in the structures than its chemical identity. Other authors have also reported the possible phase transition of the AlPO's structure by the incorporation of metals.[22,39]

4.2.1. Geometrical Changes in the $AlPO_4$-5 by the Incorporation of Iron Defects. The simulated T−O bond distances and T−O−P bond angles for the FAPO-5 are presented in Table 7. The Sayle's potential parameters predict greater distortions in the $AlPO_4$-5 framework.

(40) Schober, H.; Doner, B. *Phys. Condens. Matter* **1994**, *6*, 5351.
(41) Arias, D.; Campos, I.; Escalante, D.; Goldwasser, J.; López, C. M.; Machado, F. J.; Méndez, B.; Moronta, D.; Pinto, M.; Sazo, V.; Ramirez de Agudelo, M. M. *J. Mol. Catal.* **1997**, *122*, 175.
(42) Finger, G.; Kornatowsky, J.; Jancke, K.; Matschat, R.; Baur, W. H. *Microporous Mesoporous Mater.* **1999**, *33*, 127.

Table 6. Energy and Unit Cell Parameters for the Five Most and Least Stable Configurations with Three Fe^{3+} in the Tetrahedral Aluminum Sites of $AlPO_4$-5 Unit Cell[a]

N^b	conf			E/eV[c]	a/Å	b/Å	c/Å	α/°	β/°	γ/°
1	1	5	20	−266.5976	13.840	24.357	8.5015	89.83	90.27	90.79
2	1	2	19	−266.5968	13.823	24.426	8.5010	89.99	89.95	91.85
3	1	8	18	−266.5957	13.830	24.320	8.5069	89.78	89.88	90.59
4	1	5	19	−266.5956	13.814	24.432	8.5072	89.82	90.09	90.70
5	1	5	16	−266.5955	13.857	24.388	8.5126	90.16	90.32	89.37
251	1	5	13	−266.5749	13.854	24.258	8.5321	89.93	90.00	90.55
252	1	2	13	−266.5750	13.833	24.275	8.5247	89.96	90.05	91.45
253	1	2	9	−266.5755	13.893	24.154	8.5255	89.85	89.88	90.70
254	1	5	18	−266.5758	13.843	24.270	8.5315	89.90	89.97	89.60
255	1	22	24	−266.5758	14.073	23.942	8.5088	89.72	90.11	90.43

[a] Parameters potential of Sayle et al.[32] were used. [b] Rank by Energy. [c] Total energy per AlO_4 unit of $AlPO_4$-5.

Table 7. Fe−O Bond Distances and Fe−O−P and O−Fe−O Angles for the Substitution of One Fe^{3+} in the Orthorhombic Unit Cell of Mora et al.[7]

site	Fe−O/Å[a]	Fe−O/Å[b]	Fe−O−P/°[a]	Fe−O−P/°[b]	O−Fe−O/°[a]	O−Fe−O/°[b]
T_1	2.034−2.058	1.803−1.816	137.6−166.9	146.46−158.42	96.54−118.06	106.69−112.05
T_2	2.030−2.070	1.805−1.824	144.8−168.4	145.83−156.60	101.95−114.69	104.95−114.38
T_3	2.026−2.060	1.804−1.820	145.7−166.1	146.21−158.47	98.33−114.60	105.12−113.51
T_4	2.033−2.059	1.803−1.816	138.0−166.9	146.40−158.50	96.45−117.87	106.80−112.08
T_5	2.032−2.071	1.805−1.824	145.0−169.1	145.83−156.60	101.93−114.65	104.96−114.37
T_6	2.027−2.061	1.804−1.820	143.7−164.7	146.16−158.47	98.36−114.26	105.08−113.53

[a] Sayle et al.[32] potential parameters were used. [b] Lewis-Catlow[33] potential parameters were used.

Concerning the Fe^{3+}−O bond distances, it is observed that Fe^{3+} increases the Al−O bond distances by about 0.3 Å, which is larger than that encountered by other authors, for example, in Fe−ZSM-5.[23,24] The overestimation of the Fe^{3+} bond distances may be due to the underestimation of the short-range parameter of the Fe^{3+}−O potential by the extrapolation of the potential from an octahedral to a tetrahedral environment. However, in another EXAF study of the ZSM-5, Fe^{3+}−O bond distances of around 2.1 Å have been reported.[43] Also, the T−O−P and O−T−O angles are greatly modified as a consequence of the incorporation of Fe^{3+} ion.

The Lewis−Catlow's potential parameters produce Fe−O bond distances about ∼1.8 Å, in contrast with those obtained by Sayle's potential parameters (∼2 Å). The Fe−O bond distances are 0.1 Å larger than those experimentally reported for Al−O in $AlPO_4$-5[7] and have a good agreement with the experimental results in the Fe−ZSM-5.[24] An analysis of the T−O−P bond angles reveals an increase of about ∼2 or 3° in relation to Al−O−P in $AlPO_4$-5.[7] This increase is smaller than the one obtained with Sayle's potential parameters. Concerning the O−T-O bond angles, the influence of the incorporation of the Fe^{3+} in aluminum sites is not remarkable. According to these results, we conclude that the Lewis-Catlow's potential parameters predict more accurately the structural properties of the FAPO-5.

As a consequence of the incorporation of the Fe^{3+}, the cell parameters will also vary. This variation is strongly dependent on the substituted site. The cell volume increases (∼1−4% depending on the potential parameters used) as has been experimentally reported in other MeAPOs.[39,42] This increase has been related to the presence of the new metal in the unit cell.[39] Besides, variation in the T−O−P angles due to the incorporation of the Fe^{3+} ion in the framework results in a modification of the channel size. The maximum and minimum effective diameter of the channel varies between 0.3 and 0.8 Å depending on the substituted site. These changes would be very important for the future application of the FAPO-5 in catalytic reactions.

4.2.2. Influence of the Interaction between Defect Centers and the Geometrical Factors in the Stability of the FAPO-5. The energy difference (∼0.02 eV) between the most and the least stable configurations with one and two Fe^{3+} ions per unit cell (Tables 5 and 6) is on the order of the synthesis temperature. Thus, we would expect to find experimentally a distribution over the sites according either to the Boltzmann distribution of the measurement temperature (equilibrium) or the synthesis temperature. Moreover, we found that the stability of the FAPO-5 structure critically depends on the interactions between defects. In this respect, the dependence of the total energy on the distance between defects is shown in Figure 6. The most stable sites are those that have quasi-"noninteracting", defects and the least stable sites are the ones that have "interacting" defects. As a consequence of this fact, the structures with Fe−O−P−O−Fe units are unfavorable for the framework. Nevertheless, the analysis of the stability is, in general, more complex because of the presence of other geometrical factors in the $AlPO_4$-5 unit cell.

The behavior of all of the two and three defect configurations shows the critical effect of the unit cell constraint in the *c* direction in the Fe^{3+} incorporation (the unit cell presents more Al−O−P angles in this direction, so it is more "rigid" in this direction). Therefore, when the substitution occurs in the same side of the unit cell, the deformation in the plane *ab* of it is very strong, and the structure results unstable. In contrast, when the substitution occurs in different sides, the deformations are more appropriately accommodated in each plane of the unit cell and the structure results stable (see Figure 1c). In this sense, the 15 most stable structures of two Fe^{3+} ions correspond to configurations with one Fe^{3+} ion in one of the sides of the $AlPO_4$-5 unit cell and another defect in the opposite side. In contrast,

(43) Pataron, J.; Tuilier, M. H.; Durr, J.; Kessler, H. *Zeolites* **1992**, *12*, 70.

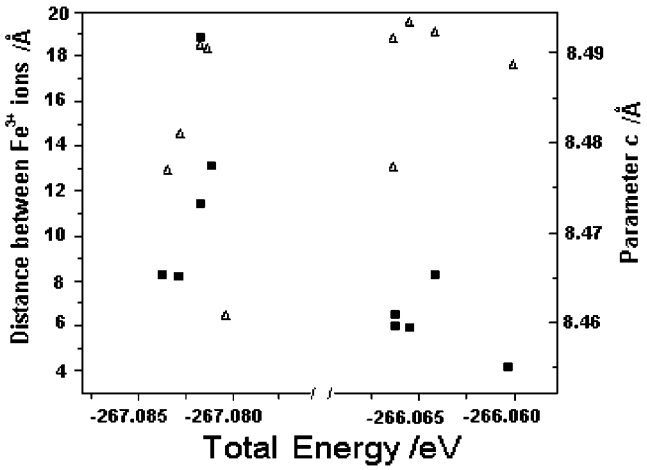

Figure 6. Dependence of the total energy on the distance between defects (close square) and on the *c* unit cell parameter (open triangle) for the five least and most stable configurations with two Fe^{3+} in aluminum tetrahedral sites of the $AlPO_4$-5 unit cell. The mean values of the *c* parameter for the five most and least stable configurations are 8.4790 and 8.4879 Å respectively.

the 15 least stable configurations have the two Fe^{3+} ions in the same side of the $AlPO_4$-5 unit cell. Finally, Figure 6 shows the correlation between the total energy per unit cell and the *c* parameter for the five least and most stable sites of two Fe^{3+} ions. As a general tendency, the five least stable configurations produce a greater increase of the *c* parameter with respect to the five most stable sites, which indicates that its crystallographic direction is essential in the $AlPO_4$-5 stability. The difference between the mean values of the *c* parameter for the five most (8.4790 Å) and least (8.4879 Å) stable configurations of two Fe^{3+}ions in aluminum tetrahedral sites is 0.008 Å. For the configurations with three Fe^{3+} ions, this difference is ∼0.02 Å. These differences can be measured in modern laboratory powder X-ray diffractometers.

Table 8. Estimation of the Interaction Energy between Defects of Fe^{3+} for Two Different Configurations

rank by energy	configuration		def. energy/eV
5	1	19	−0.09
78	9	22	0.589

Table 8 shows the interaction energy between Fe^{3+} ions for two different configurations. The interaction energy decreases as the distance between ions increases. The configuration T_9-T_{22}, the least stable of all configurations, corresponds to the case of two defects neighboring (the distance between both is 4.16 Å) and in the same side of the unit cell. In contrast, the configuration T_1-T_{19}, a very stable configuration, corresponds to the case of two defects in opposite sides of the unit cell and no neighboring (the distance between both is 13.11 Å). This example highlights the critical importance of the two factors of the structural stability of FAPO-5: the interaction between iron defects and the rigidity of the unit cell in the *c* direction.

Taking into account the previous results, the formation of a "planar" configuration of Fe^{3+} ions in $AlPO_4$-5 has a low probability. The analysis of the different configurations with three Fe^{3+} ions confirms this statement (see the five most and least stable configurations in Table 6). Of the 25 least stable configurations 80% correspond to a "planar" distribution of the Fe^{3+} in the $AlPO_4$-5 unit cell**.** The remaining 20%, corresponding to two and one Fe^{3+} ions in opposite sides, have the Fe^{3+} ions in neighboring positions. In these cases, the interaction between both neighboring defects leads to unstable structures.

Acknowledgment. We are grateful to Prof. G. B. Suffritti (Universitá degli Studi di Sassari, Italy) for his comments and critical reading of the manuscript and to Mr. R. Consuegra (Centro de Química Farmacéutica, La Habana, Cuba) for his language corrections.

CM0101428